CAMES, **27**(4): 221–239, 2020, doi: 10.24423/cames.290

Speckle Noise Reduction and Image Segmentation Based on a Modified Mean Filter

P. ARULPANDY[1)*], M. TRINITA PRICILLA[2)]

[1)] *Department of Mathematics*
Bannari Amman institute of Technology
Tamilnadu, India
*Corresponding Author e-mail: arulpandy002@gmail.com

[2)] *Department of Mathematics*
Nirmala College for Woman
Tamilnadu, India
e-mail: abishai_kennet@yahoo.in

Image segmentation is an essential process in many fields involving digital images. In general, segmentation is the process of dividing the image into objects and background image. Image segmentation is an important step in the object detection process. It becomes more critical if a given image is corrupted by noise. Most digital images are corrupted by noises such as salt and pepper noise, Gaussian noise, Poisson noise, speckle noise, etc. Speckle noise is a multiplicative noise that affects pixels in a gray-scale image, and mainly occurs in low level luminance images such as Synthetic Aperture Radar (SAR) images and Magnetic Resonance Image (MRI) images. Image enhancement is an essential task to reduce specklenoise prior to performing further image processing such as object detection, image segmentation, edge detection, etc. Here, we propose a neighborhood-based algorithm to reduce speckle noise in gray-scale images. The main aim of the noise reduction technique is to segment the noisy image. So that the proposed algorithm applies some luminance to the original image. The proposed technique performs well at maximum noise variance. Finally, the segmentation process is done by the modified mean filter. The proposed technique has three phases. In phase 1, the speckle noise is reduced and the contrast adjustment is made. In phase 2, the segmentation of the enhanced image is processed. Finally, in phase 3, the isolated pixels in the segmented image are eliminated and the final segmented image is generated. This technique does not require any threshold value to segment the image; it will be automatically calculated based on the mean value.

Keywords: image segmentation, speckle noise, image analysis, image denoising.

1. Introduction

Image segmentation is an essential task in image processing in many fields such as robotics, automation, computer vision, etc. The segmentation process di-

vides an image into the foreground (objects) and background image. It becomes critical when the given image is corrupted by noise. Image noise reduction is one of the challenging tasks in image processing. There are various kinds of noises that affect the pixels of a digital image. No unique method is available to reduce all types of noises. Gaussian noise, salt and pepper noise and speckle noise are popular noises that affect digital images frequently. In recent years, many enhancement techniques were proposed to reduce image noise by many researchers.

In recent years, many segmentation algorithms were proposed. We classify the segmentation techniques into major categories such as structure or shape-based methods, clustering methods, and thresholding methods. Shape-based methods use the histogram to analyze peaks, valleys, and curvature of gray levels [1–3]. Clustering methods are very effective in most cases, as they classify image pixels into multiple classes according to their pixel attributes. One of the main advantages of this method is the fact that we can divide an image into any number of clusters and extract the same. However, the initialization of cluster centers has remained difficult problem untill today. Qureshi and Ahamad [4] were proposed an improved image segmentation method using k-means clustering with neutrosophic logic. In 2011, an improved fuzzy c-means image segmentation algorithm was introduced by Cheng *et al.* [5]. Image thresholding is one of the simplest ways to segment the image. Many researchers have proposed various thresholding techniques to segment noisy and noise-free images. In 1979, Nobuyuki Otsu [6] proposed a threshold selection algorithm to segment images. In 1983, Rosenfield and de la Torre [1] have applied a histogram-based threshold selection algorithm to segment digital images. Many thresholding techniques were proposed for image segmentation [7–11] until today. Gai *et al.* [12] proposed specklenoise reduction of medical ultrasound images based on wavelet and Laplace mixture distribution. Also, many survey papers about specklenoise reduction and image segmentation were published by various researchers [13, 14].

In this paper, a novel image segmentation technique based on neighborhood concepts is proposed. The proposed technique has three major steps as preprocessing, main-processing and post-processing. In pre-processing, the speckle noisy image is enhanced by applying certain formulae. Speckle noise is a multiplicative noise. In fact, speckle noise has both additive and multiplicative noises. We first reduce additive noise in the given image by considering the mean value of the noisy image. Then, we use a logarithmic function to reduce multiplicative noise and exponential function to restore the original image after removing multiplicative noise. Then the segmentation process is done by the modified mean filter and the post-processing is done to eliminate the isolated pixels to get better segmentation. In Sec. 4, we have applied the proposed algorithm to real-time images and medical images to evaluate the performance of the proposed technique. In Sec. 5, we compare, the proposed technique with various segmentation

techniques such as Otsu's thresholding [6] (global thresholding) and Niblack [15], Sauvola and Pietikäinen [16], Bradley and Roth [17] (local thresholding types) by taking the popular evaluation metrics: peak signal-to-noise ratio (PSNR), mean squarred error (MSE), structural similarity index measurement (SSIM) and correlation coefficient (CoC).

1.1. Key points

Image thresholding is one of the image processing techniques used in image segmentation. Nowadays, there are many ways to achieve image segmentation. One of the advantages of the thresholding technique is its simplicity. By using simple steps, we can achieve great results. Neighborhood-based segmentation is one type of thresholding. The main purpose of this article is to segment the image corrupted by speckle noise by using only neighborhood concepts. In past years, many authors proposed different algorithms to reduce speckle noise (despeckling). Further, many segmentation algorithms were proposed by researchers. In the 1980s, J.S. Lee proposed various noise filtering techniques to remove speckle noise in digital images [18–20]. However, the segmentation of the despeckled image did not give the best results. In this article, we propose an algorithm to enhance speckle noise and segment that image at the same time. The proposed technique is not a usual despeckling process; instead of despeckling, the noisy image was enhanced to achieve optimal segmentation. For this reason, the enhancement results are not that great compared with advanced noise removal methods. Only a few research papers dealt with image segmentation of speckle noisy image [21–23] and none of the researchers used the neighborhood concept alone. However, we compared our segmentation results with popular segmentation techniques and analyzed the results.

Generally, the output of image segmentation by thresholding techniques is a binary image. Since the shape of cancer cells is important to analyze, this type of segmentation is useful in cancer detection. To analyze and identify the sea area and soil region, image segmentation is useful in SAR images. Whenever the image is corrupted by speckle noise, image segmentation becomes a challenging task. The proposed technique is useful for the above-mentioned cases.

2. Noise classification

Noise is a random signal. Noise occurs in a digital image during image acquisition, coding, transmission and processing. Noise appearance disturbs the original image information. Image enhancement is essential to perform further image processing such as segmentation and object detection. To reduce noise in images, it is important to identify the type of noise that affects the image.

According to their nature, noises are classified as Gaussian noise, Poisson noise, salt and pepper noise, speckle noise, etc. [24]. Gaussian noise arises in amplifiers and detector images. It is caused by natural sources such as thermal vibration of atoms and the discrete nature of radiation of warm objects. Poisson noise appears due to the statistical nature of electromagnetic waves such as X-rays and gamma rays. Images with Poisson noise have a random fluctuation of photons. This noise is also called quantum noise or shot noise. Salt and pepper noise is also called impulse valued noise. This type of noise affects gray levels partially, and some pixel values are replaced by either maximum or minimum gray values. Though some pixels are affected by this noise, but their neighborhood pixels may not be affected. So it is possible to reduce salt and pepper noise by the median filter. There are many other kinds of noises that may appear in some cases.

To handle these noises, various filters are available such as the mean filter, median filter, Wiener filter, neutrosophic filter, etc. Among these filters the Wiener filter is an adaptive filter since it gives optimum results in most of the times for various types of noises.

2.1. Speckle noise

Speckle noise is a multiplicative noise, it degrades images such as synthetic aperture radar (SAR) images, ultrasound medical images, tomography images, etc. It is non-uniform noise that makes images grainier. Speckle noise may be defined as a correlated signal and it is modeled as a multiplicative noise in contrast to additive Gaussian and impulse noise. Speckle noise can be modeled as follows [25]:

$$G(i,j) = g(i,j) * \gamma(i,j) + \eta(i,j), \tag{1}$$

where $G(i,j)$ is observed image, $\gamma(i,j)$ is a multiplicative noise, $g(i,j)$ is the noise-free image and $\eta(i,j)$ is additive noise.

2.2. Salt and pepper noise

Salt and pepper noise is also called impulse noise. The digital image is corrupted by noisy pixel with impulse values, i.e., maximum noise and minimum noise. However, the image is not fully corrupted by impulse values. It is possible that the neighborhood has uncorrupted pixel values. Salt and pepper noise generally corrupts digital image due to the malfunction in camera sensors, corrupted memory storage device, and errors in digitization process.

2.3. Gaussian noise

Gaussian noise is an electronic noise. It occurs mostly in electronic devices such as amplifiers and detectors. An image is affected by Gaussian noise due to the natural sources like the vibration of atoms and radiation in objects. Gaussian noise is modeled as the distribution function as follows:

$$P(g) = \sqrt{\frac{1}{2\pi\sigma^2}} e^{-\frac{(g-\mu)^2}{2\sigma^2}}, \tag{2}$$

where g is the pixel value, σ is the standard deviation and μ is the mean.

2.4. Poisson noise

Poisson noise is also called a photon noise. Because, it frequently occurs due to electromagnetic waves such as X-rays, gamma rays and visible lights. These rays are used in medical images to identify diseases by the random fluctuation of photons. This noise is also called quantum noise or shot noise. Poisson noise follows the Poisson distribution.

$$P(g) = \frac{\lambda_i^g e^{-\lambda}}{g!}. \tag{3}$$

2.5. Gamma noise

Gamma noise follows the gamma distribution. It occurs due to the low-pass filtering of laser-based images. It is modeled as:

$$P(g) = \frac{a^b g^{b-1} e^{-ag}}{(b-1)!} \quad \text{for} \quad g \geq 0, \tag{4}$$

where $\mu = \dfrac{b}{a}$, $\sigma^2 = \dfrac{b}{a^2}$ represent mean and variance, respectively.

2.6. Rayleigh noise

Rayleigh noise occurs in radar images and it is modeled as:

$$P(g) = \frac{2}{b}(g-a) e^{-\frac{(g-a)^2}{b}} \quad \text{for} \quad g \geq a, \tag{5}$$

where $\mu = a + \sqrt{\dfrac{\pi b}{4}}$, $\sigma^2 = \dfrac{b(4-\pi)}{4}$ represent mean and variance, respectively.

In the following section, we propose an algorithm to enhance speckle noise and segment gray-scale images.

3. Speckle noise

Speckle noise is a type of noise that affects the image portion gradually. Unlike other noise types, speckle noise causes uneven pixel distribution. Generally, speckle follows the gamma distribution (approximately). It occurs almost in all coherent images such as SAR images, medical ultrasound images, etc. Speckle noise is modeled as the combination of multiplicative and additive noise by the mathematical equation as follows:

$$G(i,j) = g(i,j) * \gamma(i,j) + \eta(i,j), \tag{6}$$

where $G(i,j)$ is observed image, $\gamma(i,j)$ is a multiplicative noise, $g(i,j)$ is the noise-free image and $\eta(i,j)$ is additive noise.

The graph of gamma distribution is given below (Fig. 1).

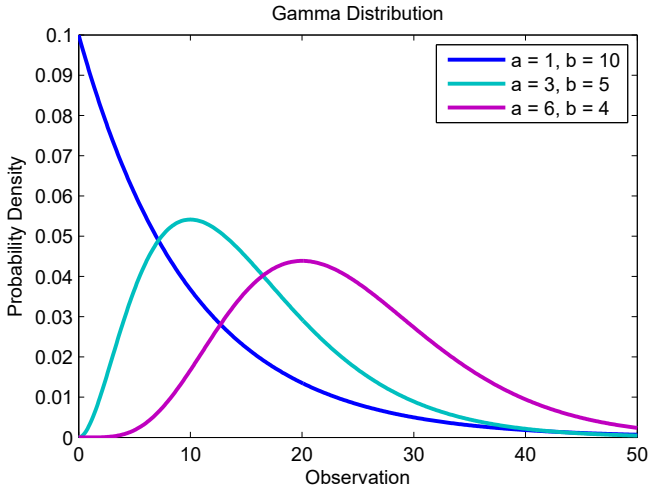

Fig. 1. The probability density function of gamma distribution.

It is possible to generate artificial speckle noise in an image using MATLAB and Python code. Since the real-time images may contain multiple noises, raw images are not useful for analytical purpose. Most of the image processing algorithms were tested on only artificial noise images generated by computer code. The SAR image with speckle noise and their pixel distributions are given in Fig. 2. Images 2a, 2b and 2c represent SAR image with speckle noise variance ($\sigma = 0.1, 0.5$) and images 2d, 2e and 2f represent their corresponding histograms. We can clearly see the similarity between histograms and the gamma distribution 1. It shows that the speckle noise follows the gamma distribution.

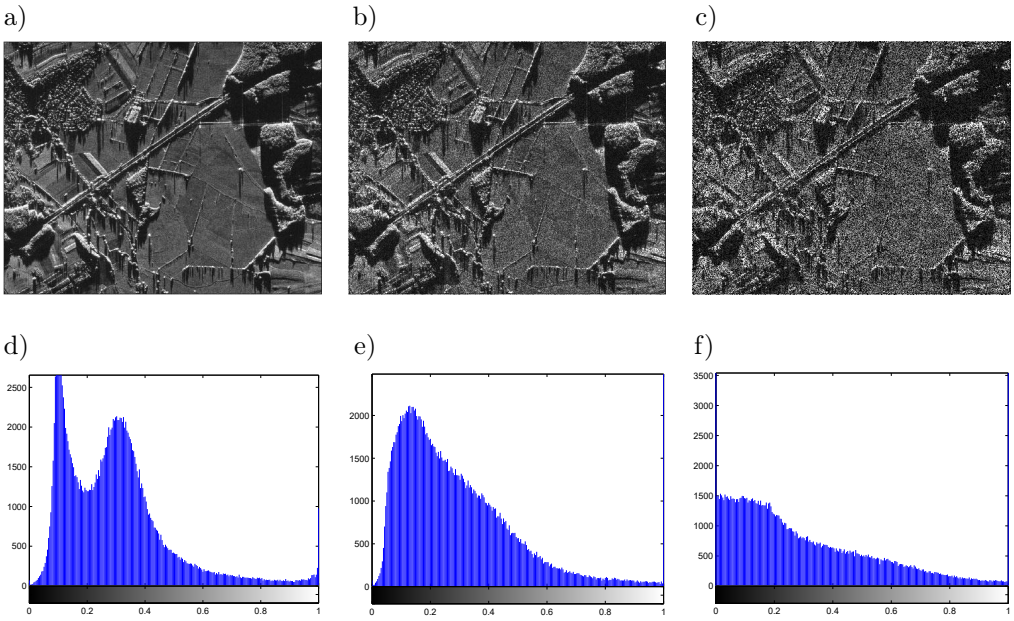

Fig. 2. SAR images with different speckle noise levels and their corresponding histograms: a) SAR image, b) SAR with speckle $\sigma = 0.1$, c) SAR with speckle $\sigma = 0.5$, d) histogram of (a), e) histogram of (b), f) histogram of (c).

4. Proposed method

Our main goal is to enhance gray-scale images by reducing the speckle noise while retaining image information as much as possible and segment the enhanced image. The proposed technique is divided into three stages. Firstly, speckle noise is reduced, and then the segmentation process is done by the modified mean filter. Finally, the segmented image is enhanced by removing isolated pixels.

4.1. Algorithm

The proposed algorithm consists of three sections: image enhancement (pre-processing), image segmentation (main-processing) and enhanced segmentation (post-processing).

Step 1
Read input image $g(i, j)$ and convert it into a gray-scale image if it is RGB. Then change image data type into double precision (i.e., pixel range 0–255 into 0–1).

Step 2
Add speckle noise to the input image $g(i, j)$ with noise variance σ.

Step 3
Define $w \times w$ neighborhood for each pixel of $g(i,j)$ of window size w. Here, we take $w = 3$:

$$W = \left\{ \left\{ g(m,n) \right\}_{m=i-w/2}^{i+w/2} \right\}_{n=j-w/2}^{j+w/2}. \tag{7}$$

Then, compute the mean value for each neighborhood window:

$$\overline{g}(i,j) = \frac{1}{w \times w} \sum_{m=i-w/2}^{i+w/2} \sum_{n=j-w/2}^{j+w/2} g(m,n). \tag{8}$$

Step 4
To reduce the additive noise, subtract the mean value $\overline{g}(i,j)$ from each neighborhood pixel for the entire image:

$$W_\alpha = W - \overline{g}(i,j) = \left\{ \left\{ g(m,n) - \overline{g} \right\}_{m=i-w/2}^{i+w/2} \right\}_{n=j-w/2}^{j+w/2}. \tag{9}$$

Step 5
To reduce the multiplicative noise, take a logarithm for W_α and enhance it by adding $\overline{g}(i,j)$:

$$W_\beta = \log(W_\alpha) + \overline{g}(i,j). \tag{10}$$

Step 6
Restore the original image by taking exponential on W_β:

$$W_\gamma = \exp(W_\beta) = e^{W_\beta}. \tag{11}$$

Step 7
The enhanced image is defined by:

$$G_{En}(i,j) = \max\left\{ \max\left\{ W_\gamma \right\}_{m=i-w/2}^{i+w/2} \right\}_{n=j-w/2}^{j+w/2}. \tag{12}$$

Step 8
The enhanced image is segmented in this step. Calculate the mean value of the entire enhanced image $G_{En}(i,j)$:

$$\overline{G}_{En}(i,j) = \text{mean}\{\text{mean}\{G_{En}\}\} = \frac{\text{Sum of pixel values}}{\text{Number of pixels}}. \tag{13}$$

The segmented image is defined by:

$$G_{Pre-Seg}(i,j) = \begin{cases} 1 & \text{if } G_{En}(i,j) > \overline{G}_{En}(i,j), \\ 0 & \text{otherwise.} \end{cases} \tag{14}$$

Step 9
To eliminate isolated pixels, the post-processing enhancement is required. Define 3×3 neighborhood for each pixel in $G_{Pre-Seg}$:

$$W_{Seg} = \left\{ \left\{ G_{Pre-Seg}(m,n) \right\}_{m=i-w/2}^{i+w/2} \right\}_{n=j-w/2}^{j+w/2}. \tag{15}$$

Also, define:
V_0 = Set of pixels has value 0 in W_{Seg},

V_1 = Set of pixels has value 1 in W_{Seg},

$N(V_0)$ = Number of pixels in V_0,

$N(V_1)$ = Number of pixels in V_1.

Step 10
The final segmented image is defined by:

$$G_{Seg}(i,j) = \begin{cases} 1 & \text{if } N(V_1) > N(V_0), \\ 0 & \text{if } N(V_1) < N(V_0). \end{cases} \tag{16}$$

5. Experimental results

In this section, the proposed image segmentation technique is applied to real-time and medical images at different speckle noise variances. The proposed segmentation algorithm is applied to the following Cameraman image with speckle noise variance $\sigma = 0.4$.

Figure 3 shows the process of the proposed technique. Firstly, the noisy image is enhanced by reducing speckle noise significantly. Here, the usual despeckling is not used since the enhanced image is only for segmentation purpose. So the contrast level of enhanced image is slightly higher than that of the original image. Figure 3a represents the original Cameraman image and Fig. 3b shows the noisy image at speckle noise variance $\sigma = 0.4$. Figure 3c shows the enhanced image and Fig. 3d represents the (pre)segmented image. Note that the image 3d contains lots of isolated pixels. So post-processing is needed to remove those pixels. Figure 3e represents the final segmented image after enhancement.

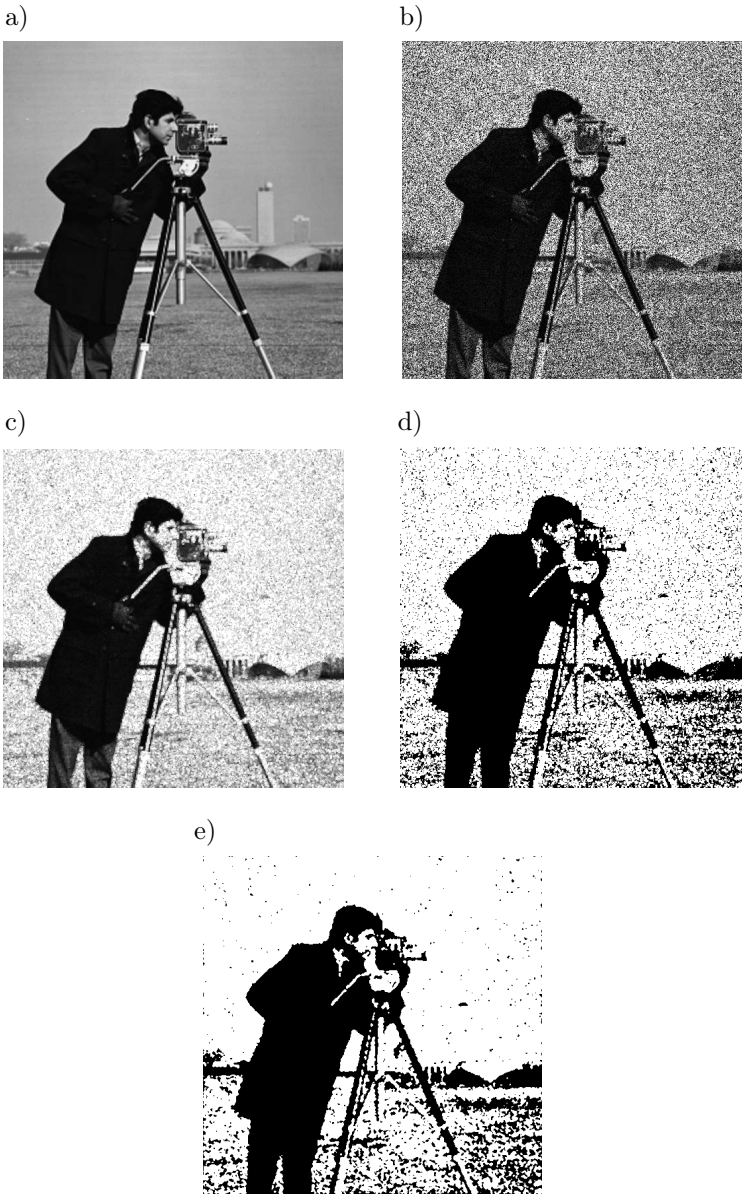

Fig. 3. Cameraman image segmented by the proposed technique: a) original image, b) speckle noisy image ($\sigma = 0.4$), c) enhanced image, d) pre-segmented image, e) final segmented image.

To evaluate the significance of the proposed algorithm, the real-time image (House image) and medical image (MRI) are processed through the proposed technique at different noise levels. Figure 4 shows that the enhanced and segmented House image at various speckle noise levels. Figure 5 shows the enhancement and segmentation of MRI medical image.

Noisy image Enhanced image Segmented image

a) Speckle noise with variance $\sigma = 0.2$

b) Speckle noise with variance $\sigma = 0.4$

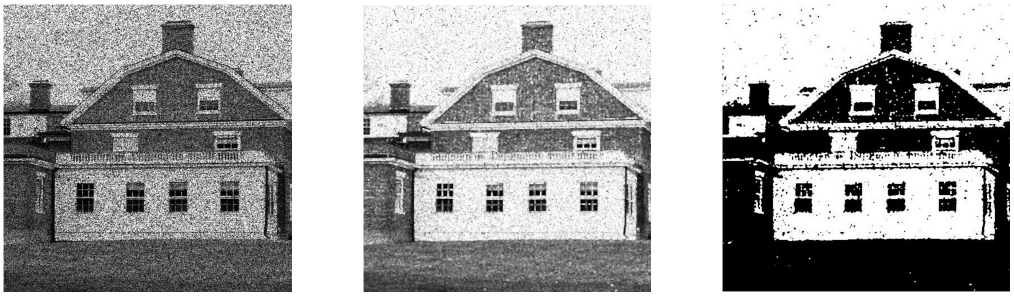

c) Speckle noise with variance $\sigma = 0.6$

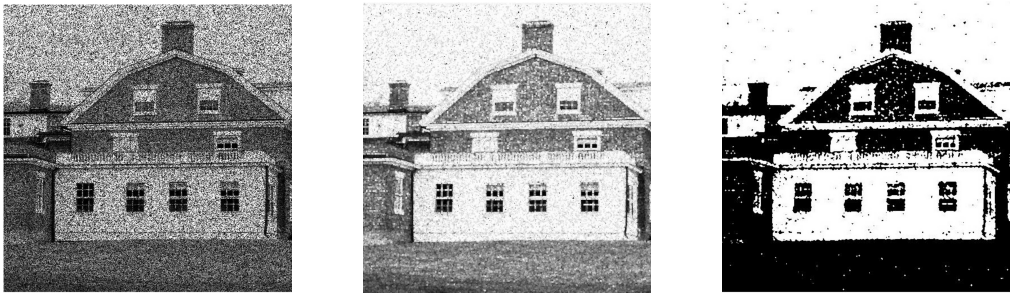

d) Speckle noise with variance $\sigma = 0.8$

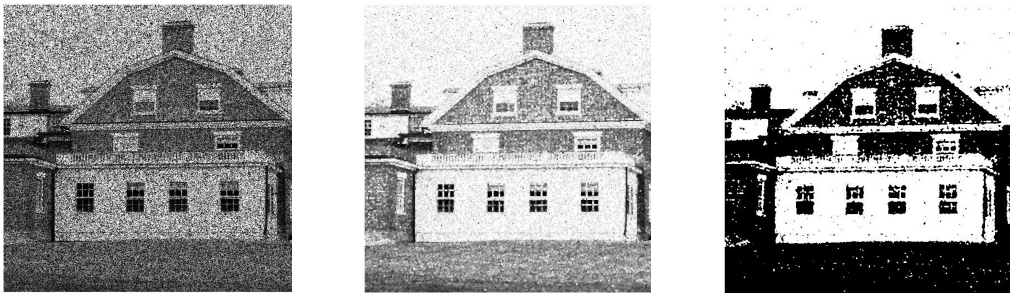

FIG. 4. Speckle noise enhancement and segmentation of House image at different noise levels.

Noisy image Enhanced image Segmented image

a) Speckle noise with variance $\sigma = 0.2$

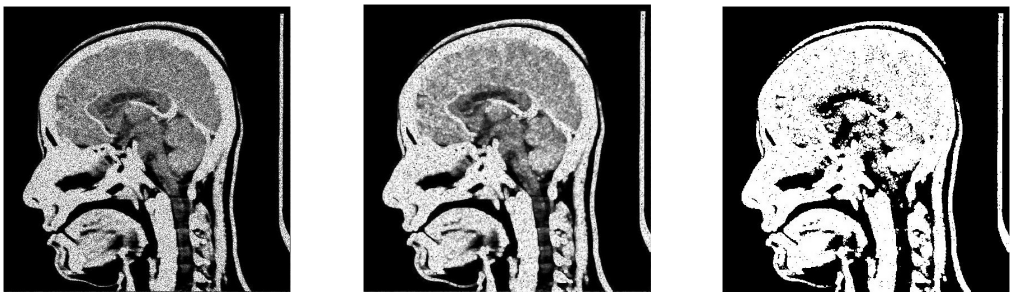

b) Speckle noise with variance $\sigma = 0.4$

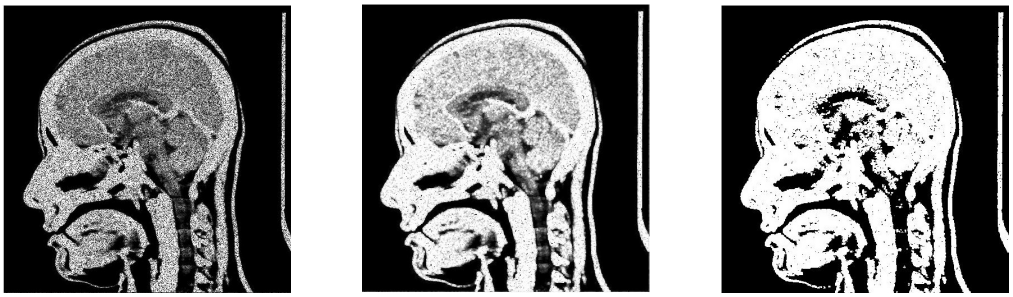

c) Speckle noise with variance $\sigma = 0.6$

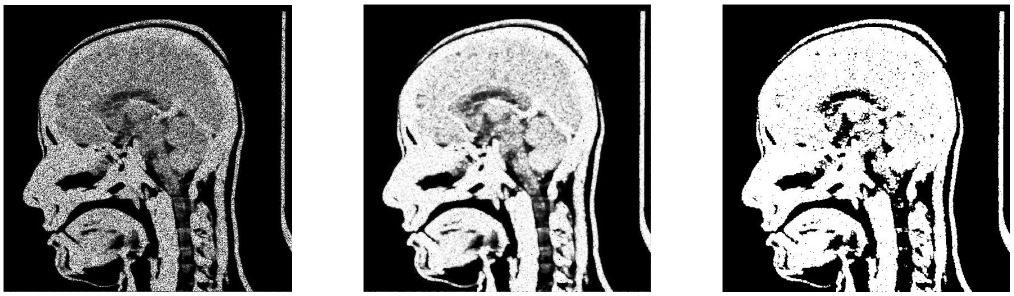

d) Speckle noise with variance $\sigma = 0.8$

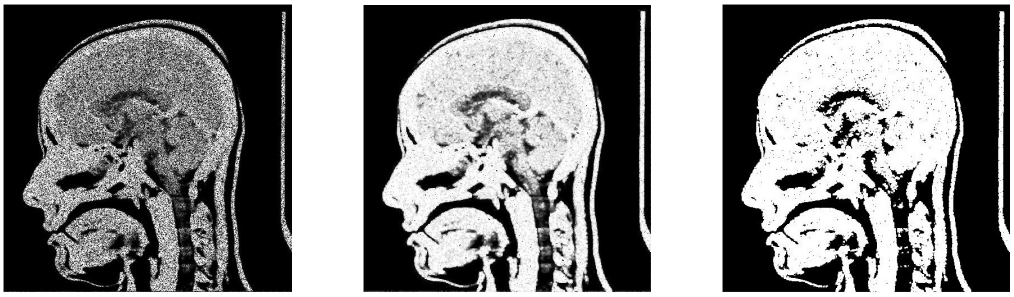

FIG. 5. Speckle noise enhancement and segmentation of MRI (head) image at different noise levels.

6. Performance evaluation

In this section, the performances of various segmentation techniques are compared with the proposed technique. In fact, there is no standard benchmark to evaluate the segmentation algorithm for all kinds. However, there are many metrics available to compare image quality and structure based on noise ratio, structure, connectivity, edge preservation, etc. Here, the results of various segmentation techniques are analyzed by the metrics: peak signal-to-noise ratio (PSNR), mean squarred error (MSE), structural similarity index measurement (SSIM) and correlation coefficient (CoC).

PSNR and MSE metrics are generally used to measure the quality of an image after noise removal. High PSNR value means the best quality of enhancement and low PSNR value shows the low quality of enhancement. Similarly, MSE is used to measure the errors between two similar images (original and enhanced images). High MSE values show the low quality and low MSE values show the high quality enhancement:

$$\mathrm{PSNR} = -10\log\left[\frac{\sum_{i=0}^{m-1}\sum_{j=0}^{n-1}[G(i,j)-S(i,j)]^2}{m\times n\times 255^2}\right], \tag{17}$$

$$\mathrm{MSE} = \frac{\sum_{i=0}^{m-1}\sum_{j=0}^{n-1}[G(i,j)-S(i,j)]^2}{m\times n}. \tag{18}$$

The SSIM was proposed by Zhou Wang *et al.* [26] in 2004. SSIM is a metric used to measure the structural information such as luminance (l), contrast (c) and structure (s) and is defined as:

$$\mathrm{SSIM} = \frac{(2\mu_f\mu_g + c_1)(2\sigma_{fg} + c_2)}{(\mu_f^2 + \mu_g^2 + c_1)(\sigma_f^2 + \sigma_g^2 + c_2)}, \tag{19}$$

where μ_f, μ_g are the mean values of the original and segmented image, respectively. Also, σ_f, σ_g are the variance of the original and segmented image, respectively. σ_{fg} is the covariance of images f and g, and c_1, c_2 are two variables to stabilize the division with a weak denominator.

Correlation co-efficient is used to measure the similarity between two images. Generally, CoC values ranges from 0 to 1 (i.e., 0 means no similarity and 1 means maximum similarity). CoC is defined as follows:

$$\rho = \frac{\frac{1}{n^2}\sum_{i=1}^{m}\sum_{j=1}^{n}\big(g(i,j)-\overline{g}(i,j)\big)\big(s(i,j)-\overline{s}(i,j)\big)}{\sqrt{\frac{1}{n^2}\sum_{i=1}^{m}\sum_{j=1}^{n}\big(g(i,j)-\overline{g}(i,j)^2\big)}\sqrt{\frac{1}{n^2}\sum_{i=1}^{m}\sum_{j=1}^{n}\big(s(i,j)-\overline{s}(i,j)^2\big)}}, \tag{20}$$

where $g(i,j)$, $s(i,j)$ represent the original image and segmented image, respectively, and $\overline{g}(i,j)$, $\overline{s}(i,j)$ represent the mean values of the original image and segmented image, respectively.

Here, we compare the proposed technique with conventional segmentation techniques. Various thresholding segmentation techniques are considered. Global thresholding is one of the popular and simple thresholding methods. Otsu's thres-

Table 1. PSNR values of the images segmented by various techniques.

Noise Variance σ	Images	PSNR Values				
		[15]	[16]	[17]	[6]	Proposed
0.1	House	5.0572	5.1236	5.8743	10.2991	11.5127
	Head (MRI)	4.1698	4.9318	6.7361	9.7381	8.9858
	Cameraman	4.6176	5.2895	6.0448	8.9825	10.5912
0.2	House	5.0032	5.0712	5.7982	10.7035	11.9081
	Head (MRI)	4.1394	4.9318	6.7361	9.7384	8.9858
	Cameraman	4.5228	5.2112	6.0193	8.6507	10.8655
0.3	House	4.9899	5.0501	5.7455	10.6501	11.9728
	Head (MRI)	4.0772	4.8624	6.6430	8.8501	8.8687
	Cameraman	4.2512	5.1550	6.0143	8.3208	10.5131
0.4	House	4.9737	5.0137	5.6403	10.2458	11.9372
	Head (MRI)	4.1544	4.9416	6.7385	8.6212	8.7789
	Cameraman	4.0344	5.0973	5.9433	8.1115	10.1321
0.5	House	4.9305	5.0188	5.5672	9.6258	11.7493
	Head (MRI)	4.0428	4.8818	6.5914	8.4809	8.6743
	Cameraman	3.8815	5.0579	5.9389	7.9750	9.6388
0.6	House	4.9139	5.0187	5.5052	9.1939	11.5852
	Head (MRI)	4.0371	4.9282	6.3879	8.3809	8.5814
	Cameraman	3.7822	5.0293	5.9453	7.9036	9.2690
0.7	House	4.8989	5.0251	5.4090	8.5998	11.2335
	Head (MRI)	3.9856	4.9252	6.3293	8.2792	8.4717
	Cameraman	3.6630	4.9984	5.9361	7.7568	9.0130
0.8	House	4.8720	5.0408	5.3409	8.0235	11.0983
	Head (MRI)	3.9347	4.9660	6.2106	8.2131	8.4016
	Cameraman	3.5775	4.9753	5.9840	7.7399	8.7916
0.9	House	4.8355	5.0394	5.2783	7.4383	10.7814
	Head (MRI)	3.9657	4.9154	6.1084	8.1510	8.3271
	Cameraman	3.5015	4.9591	5.9892	7.6706	8.5972

holding [6] is based on the global thresholding technique. Local thresholding techniques are also used for segmentation. In local thresholding, the threshold value is defined locally. This means, that the value dynamically changes at every neighborhood. Here, we consider the local thresholding methods such as Niblack thresholding [15], Sauvola and Pietikäinen thresholding [16] and Bradley and Roth thresholding [17] for performance evaluation.

Tables 1 and 2 show the comparison of PSNR and MSE values of the images segmented by different segmentation techniques.

Table 2. MSE values of the images segmented by various techniques.

Noise Variance σ	Images	MSE Values				
		[15]	[16]	[17]	[6]	Proposed
0.1	House	0.3946	0.3871	0.3097	0.0933	0.0706
	Head (MRI)	0.3828	0.3212	0.2120	0.1062	0.1263
	Cameraman	0.3689	0.2940	0.3453	0.1264	0.0873
0.2	House	0.4008	0.3930	0.3170	0.0850	0.0644
	Head (MRI)	0.3855	0.3230	0.2085	0.1211	0.1279
	Cameraman	0.3774	0.2963	0.3530	0.1364	0.0819
0.3	House	0.4024	0.3954	0.3221	0.0861	0.0635
	Head (MRI)	0.3911	0.3264	0.2166	0.1303	0.1298
	Cameraman	0.3836	0.2968	0.3757	0.1472	0.0889
0.4	House	0.4042	0.3996	0.3325	0.0945	0.0640
	Head (MRI)	0.3842	0.3205	0.2119	0.1374	0.1325
	Cameraman	0.3901	0.3033	0.3950	0.1545	0.0970
0.5	House	0.4093	0.3990	0.3398	0.1090	0.0668
	Head (MRI)	0.3942	0.3250	0.2192	0.1419	0.1357
	Cameraman	0.3946	0.3037	0.4091	0.1594	0.1087
0.6	House	0.4112	0.3990	0.3461	0.1204	0.0694
	Head (MRI)	0.3947	0.3215	0.2297	0.1452	0.1386
	Cameraman	0.3978	0.3032	0.4186	0.1620	0.1183
0.7	House	0.4130	0.3983	0.3561	0.1380	0.0753
	Head (MRI)	0.3994	0.3217	0.2328	0.1486	0.1422
	Cameraman	0.4014	0.3040	0.4302	0.1676	0.1255
0.8	House	0.4162	0.3965	0.3634	0.1576	0.0777
	Head (MRI)	0.4041	0.3187	0.2393	0.1509	0.1445
	Cameraman	0.4040	0.2996	0.4388	0.1683	0.1321
0.9	House	0.4205	0.3967	0.3701	0.1804	0.0835
	Head (MRI)	0.4013	0.3224	0.2450	0.1531	0.1470
	Cameraman	0.4059	0.2991	0.4465	0.1710	0.1381

Figures 6–8 show the chart comparing PSNR and MSE values of house, MRI (head) and cameraman segmented images, respectively.

Table 3 shows the SSIM and CoC values of different images segmented by various techniques at different noise levels.

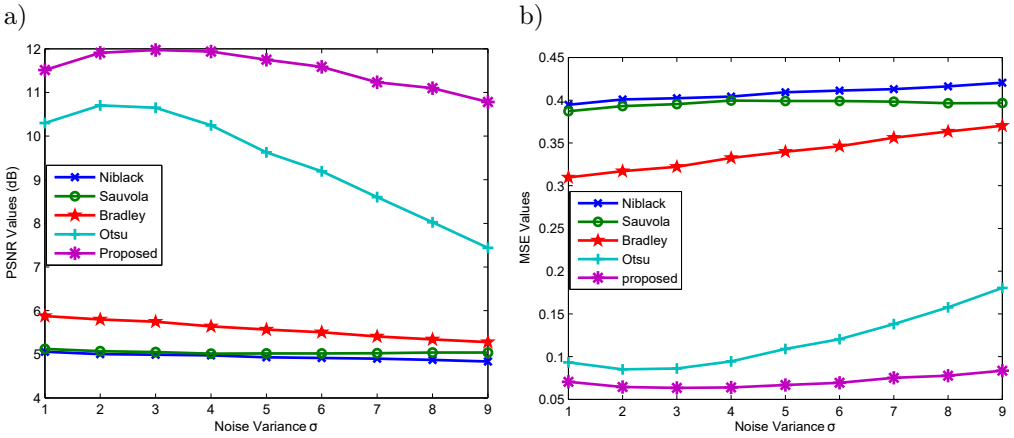

FIG. 6. PSNR and MSE comparison of house segmented image.

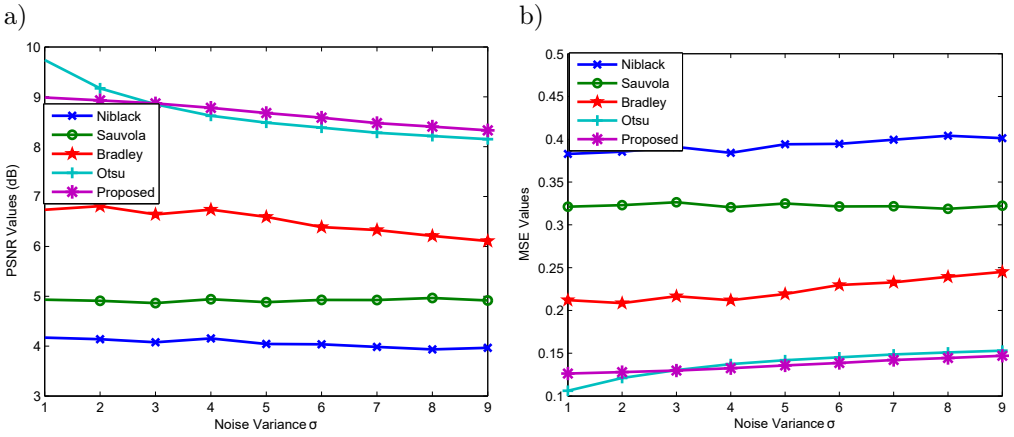

FIG. 7. PSNR and MSE comparison of head (MRI) segmented image.

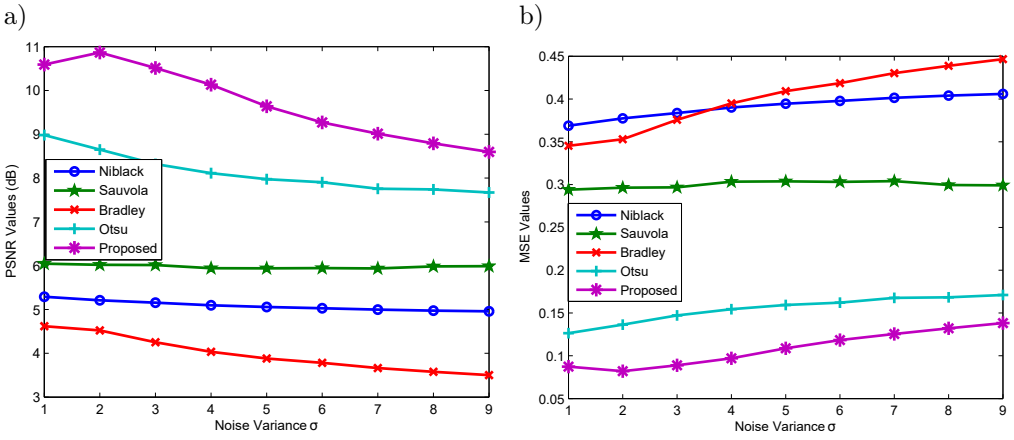

FIG. 8. PSNR and MSE comparison of cameraman segmented image.

Table 3. SSIM and CoC values of images segmented by various techniques.

Noise Variance σ	Images	[15]		[16]		[17]		[6]		Proposed	
		SSIM	CoC	SSIM	CoC	SSIM	CoC	SSIM	CoC	SSIM	CoC
0.1	a	96.5304	0.4016	94.6433	0.5043	96.8990	0.5958	99.6421	0.8153	99.6675	0.8634
	b	97.5413	0.3101	97.2332	0.4692	98.7367	0.5499	99.4173	0.7869	99.1146	0.7601
	c	96.9178	0.3379	95.7727	0.4140	97.6046	0.5740	99.2947	0.7427	99.547	0.8195
0.2	a	96.4551	0.3965	94.5378	0.4865	96.7436	0.5803	99.6702	0.8316	99.7114	0.8741
	b	97.5107	0.3046	97.1832	0.4696	98.7510	0.5579	99.1338	0.7689	99.0295	0.7594
	c	96.8054	0.3227	95.6979	0.4048	97.5036	0.5585	99.0550	0.7279	99.6571	0.8303
0.3	a	96.4418	0.3815	94.4771	0.4815	96.6934	0.5698	99.6312	0.8321	99.7190	0.8760
	b	97.4692	0.3943	97.1298	0.4699	98.6445	0.5434	98.9792	0.7562	98.9867	0.7570
	c	96.7386	0.3121	95.6379	0.4032	97.2690	0.5154	98.8342	0.7109	99.5600	0.8174
0.4	a	96.4231	0.3763	94.4267	0.4663	96.5687	0.5488	99.5571	0.8182	99.7155	0.8750
	b	97.5734	0.3012	97.2087	0.4726	98.7103	0.5490	98.8618	0.7463	98.9326	0.7532
	c	96.6679	0.2891	95.6417	0.3761	97.0530	0.4783	98.7042	0.6985	99.4558	0.8024
0.5	a	96.3645	0.3760	94.4531	0.4679	96.4805	0.5335	99.4259	0.7947	99.6858	0.8706
	b	97.4383	0.3832	97.1629	0.4676	98.6372	0.5362	98.7950	0.7400	98.8824	0.7485
	c	96.6238	0.2774	95.6338	0.3741	96.8887	0.4495	98.6246	0.6903	99.2985	0.7812
0.6	a	96.3410	0.3584	94.4483	0.4684	96.4084	0.5201	99.3183	0.7762	99.6609	0.8665
	b	97.4677	0.3782	97.1707	0.4770	98.5169	0.5159	98.7427	0.7357	98.8358	0.7449
	c	96.5915	0.2712	95.6229	0.3762	96.7811	0.4304	98.5798	0.6855	99.1604	0.7639
0.7	a	96.3178	0.3372	94.4539	0.4719	96.2967	0.4996	99.1655	0.7477	99.6105	0.8564
	b	97.4166	0.3688	97.1718	0.4767	98.4770	0.5078	98.6912	0.7308	98.7813	0.7397
	c	96.5680	0.2689	95.6181	0.3725	96.6422	0.4061	98.5040	0.6756	99.0583	0.7515
0.8	a	96.2842	0.3210	94.4514	0.4810	96.2163	0.4845	98.9722	0.7167	99.5981	0.8520
	b	97.3555	0.3588	97.1826	0.4848	98.4243	0.4929	98.6657	0.7273	98.7527	0.7364
	c	96.5355	0.2312	95.6154	0.2909	96.5468	0.3896	98.4984	0.6745	98.9612	0.7403
0.9	a	96.2249	0.3112	94.4400	0.4812	96.1237	0.4708	98.7219	0.6812	99.5635	0.8411
	b	97.3843	0.3611	97.1830	0.4750	98.3665	0.4797	98.6337	0.7243	98.7181	0.7326
	c	96.5144	0.2293	95.6041	0.2930	96.4727	0.3739	98.4616	0.6695	98.8693	0.7296

a – House, b – Head (MRI), c – Cameraman.

From Table 3, we conclude that the performance of the proposed technique is superior to the other techniques. The three images: house, MRI and cameraman are segmented by various techniques and evaluated with different metrics such as PSNR, MSE, SSIM and CoC. By these scores, the proposed technique performs well with speckle noise at any variance level.

7. Conclusion

Image segmentation is one of the important tasks in every field that deals with digital images. Segmentation becomes critical whenever the given images

were corrupted by noise. In this paper, we have proposed an algorithm to enhance speckle noise and segment the enhanced image. The proposed technique was applied to real-time and medical images at different speckle noise variance levels. The experimental results show the efficiency of our proposed method. Further, we have analyzed the performance of the proposed method with other conventional segmentation techniques and the performance was evaluated by the popular metrics: PSNR, MSE, SSIM and CoC. Our future work will include image segmentation of digital images corrupted by other noises.

References

1. A. Rosenfeld, P. de la Torre, Histogram concavity analysis as an aid in threshold selection, *IEEE Transactions on Systems Man and Cybernetics*, **13**(2): 231–235, 1983, doi: 10.1109/TSMC.1983.6313118.

2. J.S. Weszka, A. Rosenfeld, Histogram modification for threshold selection, *IEEE Transactions on Systems Man and Cybernetics*, **9**(1): 38–52, 1979, doi: 10.1109/TSMC.1979.4310072.

3. M. Zhang, L. Zhang, H.D. Cheng, A neutrosophic approach to image segmentation based on watershed method, *Signal Processing*, **90**(5): 1510–1517, 2010, doi: 10.1016/j.sigpro.2009.10.021.

4. M.N. Qureshi, M.V. Ahamad, An improved method for image segmentation using k-means clustering with neutrosophic logic, *Procedia Computer Science*, **132**(7): 534–540, 2018, doi: 0.1016/j.procs.2018.05.006.

5. H.D. Cheng, Y. Guo, Y. Zhang, A novel image segmentation approach based on neutrosophic set and improved fuzzy c-means algorithm, *Neural Mathematics and Natural Computation*, **7**(1): 155–171, 2011, doi: 10.1142/S1793005711001858.

6. N. Otsu, A threshold selection method from gray-level histograms, *IEEE Transactions on Systems, Man, and Cybernetics*, **9**(1): 62–66, 1979, doi: 10.1109/TSMC.1979.4310076.

7. J.-M. Sung, D.-C. Kim, Y.-H. Ha, Image thresholding using standard deviation, Proceeding SPIE: Image Processing: Machine Vision Applications VII, 90240R, 2014, doi: 10.1117/12.2040990.

8. N. Sang, H. Li, W. Peng, T. Zhang, Knowledge-based adaptive thresholding segmentation of digital subtraction angiography images, *Image and Vision Computing*, **25**(8): 1263–1270, 2007, doi: 10.1016/j.imavis.2006.07.026.

9. P.L. Rosin, E. Ioannidis, Evaluation of global image thresholding for change detection, *Pattern Recognition Letters*, **24**(14): 2345–2356, 2003, doi: 10.1016/S0167-8655(03)00060-6.

10. Z. Li, Y. Cheng, C. Liu, C. Zhao, Minimum standard deviation difference-based thresholding, *International Conference on Measuring Technology and Mechatronics Automation*, 2: 664–667, 2010, doi: 10.1109/ICMTMA.2010.579.

11. Z. Hou, Q. Hu, W. Nowinski, On minimum variance thresholding, *Pattern Recognition Letters*, **27**(14): 1732–1743, 2006, doi: 10.1016/j.patrec.2006.04.012.

12. S. Gai, B. Zhang, C. Yang, L. Yu, Speckle noise reduction in medical ultrasound image using monogenic wavelet and Laplace mixture distribution,*Digital Signal Processing*, **72**: 192–207, 2018, doi: 10.1016/j.dsp.2017.10.006.

13. M. Sezgin, B. Sankur, Survey over image thresholding techniques and quantitative performance evaluation, *Journal of Electronic Imaging*, **13**(1): 146–165, 2004, doi: 10.1117/1.1631315.

14. J. Jaybhay, R. Shastri, A study of speckle noise reduction filters, *Signal and Image Processing: An International Journal*, **6**(3): 71–80, 2015, doi: 10.5121/sipij.2015.6306.

15. W. Niblack, *An introduction to digital image processing*, Prentice Hall Publishers, 1986.

16. J. Sauvola, M. Pietikäinen, Adaptive document image binarization, *Pattern Recognition*, **33**(2): 225–236, 2000, doi: 10.1016/S0031-3203(99)00055-2.

17. D. Bradley, G. Roth, Adaptive thresholding using integral image, *Journal of Graphics Tools*, **12**(2): 13–21, 2007, doi: 10.1080/2151237X.2007.10129236.

18. J.-S. Lee, Digital image enhancement and noise filtering by use of local statistics, *IEEE Transactions on Pattern Analysis And Machine Intelligence*, **2**(2): 165–168, 1980, doi: 10.1109/TPAMI.1980.4766994.

19. J.-S. Lee, Speckle analysis and smoothing of synthetic aperture radar images, *Computer Graphics and Image Processing*, **17**(1): 24–32, 1981, doi: 10.1016/S0146-664X(81)80005-6.

20. J.-S. Lee, Refined filtering of image noise using local statistics, Computer Graphics and Image Processing, **15**(4): 380–389, 1981, doi: 10.1016/S0146-664X(81)80018-4.

21. J. Senthilnath, H.V. Shenoy, R. Rajendra, S.N. Omkar, V. Mani, P.G. Diwakar, Integration of speckle de-noising and image segmentation using synthetic aperture radar image for flood extent extraction, *Journal of Earth System Science*, **122**: 559–572, 2013, doi: 10.1007/s12040-013-0305-z.

22. V.P. Kharchenko, N.S. Kuzmenko, I.V. Ostroumov, An investigation of synthetic aperture radar speckle filtering and image segmentation considering wavelet decomposition, 2019 European Microwave Conference in Central Europe (EuMCE), pp. 398–401, May 2019.

23. X. Li, D.C. Liu, Ultrasound speckle reduction based on image segmentation and diffused region growing, [in:] *11th Joint International Conference on Information Sciences*, pp. 338–344, 2008, doi: 10.2991/jcis.2008.58.

24. A.K. Boyat, B.K. Joshi, A review paper: Noise models in digital image processing, *Signal and Image Processing: An International Journal*, **6**(2): 63–75, 2015, doi: 10.5121/sipij.2015.6206.

25. J.-M. Park, W.J. Song, W. Pearlman, Speckle filtering of SAR images based on adaptive windowing, *IEEE Proceedings – Vision, Image and Signal Processing*, **146**(4): 191–197, 1999, doi: 10.1049/ip-vis:19990550.

26. Zhou Wang, A.C. Bovik, H.R. Sheikh, E. P. Simoncelli, Image quality assessment: from error visibility to structural similarity, *IEEE transactions on image processing*, **13**(4): 600–612, 2004, doi: 10.1109/TIP.2003.819861.

Received April 17, 2020; revised version August 3, 2020.